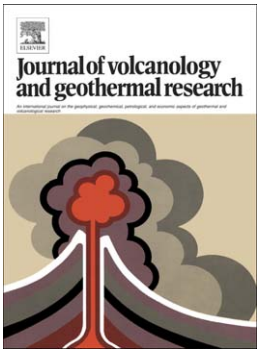

Viscosity of andesite melts and its implication for magma mixing prior to Unzen 1991–1995 eruption

Francesco Vetere, Harald Behrens, Jan A. Schuessler, Francois Holtz, Valeria Misiti, L. Borchers

PII: S0377-0273(08)00156-X
DOI: doi: 10.1016/j.jvolgeores.2008.03.028
Reference: VOLGEO 3956

To appear in: *Journal of Volcanology and Geothermal Research*

Accepted date: 24 March 2008

Please cite this article as: Vetere, Francesco, Behrens, Harald, Schuessler, Jan A., Holtz, Francois, Misiti, Valeria, Borchers, L., Viscosity of andesite melts and its implication for magma mixing prior to Unzen 1991–1995 eruption, *Journal of Volcanology and Geothermal Research* (2008), doi: 10.1016/j.jvolgeores.2008.03.028

Viscosity of andesite melts and its implication for magma mixing prior to Unzen 1991-1995 eruption

Francesco Vetere[1§], Harald Behrens[1*], Jan A. Schuessler[1], Francois Holtz[1], Valeria Misiti[2] , L. Borchers[3]

[1]Institut für Mineralogie, Universität Hannover, Callinstr. 3, D-30167 Hannover, Germany.

[2]Istituto Nazionale di Geofisica e Vulcanologia (INGV) via di Vigna Murata 605, I-00143 Roma, Italy.

[3]Poliklinik für Zahnärztliche Prothetik, Medizinische Hochschule, Carl-Neuberg-Str. 1, D-30625 Hannover, Germany.

Submitted to *Journal of Volcanology and Geothermal Research* (Unzen special issue) at octobre 31, 2005, revised at Jun1 1, 2006

* Author for correspondence:

Harald Behrens

Institut für Mineralogie, Universität Hannover, Callinstr. 3, D-30167 Hannover, Germany.

Phone: +49(0)511 762 8054

Fax: +49(0)511 762 3045

e-mail: h.behrens@mineralogie.uni-hannover.de

§ Present address: Università della Calabria, via P. Bucci I-87036 Arcavacata di Rende (CS) Italy.

Keywords: viscosity, andesite melt, dissolved water, redox state of iron, Unzen, magma mixing.

Abstract

The viscosity of an iron-bearing melt with composition similar to Unzen andesite was determined experimentally in the high (10^9-$10^{10.5}$ Pa·s) and low (5-1000 Pa·s) viscosity range using a parallel plate viscometer and the falling sphere method, respectively. Falling sphere experiments were carried out in an internally heated argon pressure vessel and in a piston cylinder apparatus at 1323 to 1573 K and 200 to 2000 MPa. Creep experiments were performed in the temperature range of 747 - 845 K at 300 MPa. The water content of the melt varies from nominally dry to 6.2 wt% H_2O. The Fe^{2+}/Fe_{tot} ratio was determined for each sample in the quenched glass using a colorimetric method. Pressure has minor influence on the viscosity compared with the effect of temperature, water content (main compositional parameter controlling the viscosity) or with the Fe^{2+}/Fe_{tot} ratio (especially important at low water content of the melt). Based on our new viscosity data and literature data with measured Fe^{2+}/Fe_{tot} ratio we propose a new empirical equation to estimate the viscosity η (in Pa·s) of andesitic melts as a function of temperature T (in K), water content w (in wt%) and Fe^{2+}/Fe_{tot} ratio. The derived relationship reproduces the experimental data (87 in total) in the viscosity range from $10^{0.5}$ to 10^{13} Pa·s with a 1σ standard deviation of 0.17 log units. However, application of this calculation model is limited to $Fe^{2+}/Fe_{tot}>0.3$ and to temperatures above T_g. Moreover, in the high viscosity range the variation of viscosity with water content is constrained only by few experimental data and needs verification by additional measurements.

The viscosity data are used to interpret mixing processes in the Unzen magma chamber prior to 1991-1995 eruption. We demonstrate that the viscosities of the rhyolite and andesite melts from the two end-member magmas are nearly identical prior and during mixing, enabling efficient magma mixing.

1. Introduction

There is strong petrological and geochemical evidence that magma mixing occurred prior to the 1991-95 eruptions of Unzen volcano (e.g., Nakada and Motomura, 1999) and it has been suggested that injection of a high temperature andesitic melt in a highly crystalline magma chamber with rhyolitic melts has initiated the eruption (e.g., Nakada and Motomura, 1999; Venezky and Rutherford, 1999; Holtz et al., 2005). On the other hand, the groundmass composition of the volcanic rocks, which was interpreted to be representative of the melt composition after mixing, is particularly homogeneous (Nakada and Motomura, 1999; Sato et al., 1999), indicating that the mixing between rhyolitic and andesitic melts must have been very efficient. Because the mixing efficiency of two liquids is mainly depending on their respective viscosities, the examination of magmatic processes occurring at Unzen needs to take into account the crucial role of melt and magma viscosity.

The main parameters which govern the viscosity of magmas are bulk composition of the melt (in particular the water content) and temperature (Bottinga and Weill, 1972; Shaw, 1972; Persikov, 1991; Giordano and Dingwell, 2003), but also pressure (Kushiro et al., 1976; Scarfe et al., 1987; Behrens and Schulze, 2003), dispersed crystals (Lejeune and Richet, 1995; Bouhifd et al, 2004; Sato, 2005) and bubbles (Lejeune et al., 1999) may have an important influence. For volcanism related to subduction zones, melts of rhyolitic to andesitic compositions are of particular interest. An extensive amount of work has been devoted to silicic systems in the last decade (see Giordano et al. 2004b and references therein). However, few studies on the viscosity of andesitic melts are available only. Except for a recent study of Vetere et al. (2006), no systematic dataset was obtained in the low viscosity range. Using data of Richet et al. (1996) and Liebske et al. (2003) obtained in the high

viscosity range, Vetere et al., (2006) proposed a model for calculating andesite melt viscosities over the range 10^1 to 10^{12} Pa·s. This model is based only on data for analogue compositions in which iron was replaced by Mg, Ca and Al to avoid experimental problems in controlling the redox state of iron and avoiding loss of iron from the melt during experiment. The question is whether the model can be directly applied to natural melt compositions at geological relevant conditions.

In this paper we want to enrich the dataset on viscosity of Fe-bearing andesitic melts especially in the high temperature range. Natural andesitic melts at high pressure may contain up to 10 wt% of dissolved H_2O (Grove et al., 2003) which strongly decreases the viscosity compared to the dry melt. Hence, a major focus of our work is on the effect of dissolved water on melt viscosity. Liebske et al. (2003) demonstrated that the viscosity of dry andesitic melts above the glass transition can decrease by about 1.6 log unit when the Fe^{2+}/Fe_{tot} ratio increases from 0.42 to 0.79. The effect of redox state of iron may be different at high temperature and at high water content of the melt. Hence, controlling and varying Fe^{2+}/Fe_{tot} were important issues in our study. The viscosity was investigated over a wide range of temperature and pressure using the falling sphere(s) method (in the range 5-10^3 Pa·s) and the creep method (in the range 10^9-$10^{10.5}$ Pa·s). The new experimental data on melt viscosity are used to discuss mixing processes between felsic and andesitic melts in the Unzen magma chamber prior to 1991-1995 eruption.

2. Experimental and Analytical Methods

2.1. Starting materials

The starting composition is based on an andesite from Unzen Volcano (Pre Unzen 500 kyr; Chen et al., 1993). Two dry glasses were synthesized, labelled as compositions MDIB1 and MDIB2 in Table 1. In each synthesis about 100 g of glass was produced by melting a mixture of oxides and carbonates at 1873 K for 4 h in a Pt crucible in air. Part of the melt was quenched by pouring on a brass plate. A large part of the melt, however, stuck in the crucible and was quenched by dropping the crucible into water. To improve homogeneity, the glass was crushed, re-melted and quenched at same conditions. The poured glass was used for microprobe analyses. The glass stuck at the wall was crushed and used for preparation of viscosity samples.

The most oxidized water-poor samples for viscosity experiments were produced by re-melting of compacted glass powder in AuPd capsule for 20 h at 1523 K, 500 MPa in the internally heated gas pressure vessel (IHPV). The air-melted glass could not be used directly for viscosity experiments because the Fe^{2+}/Fe_{tot} ratio is much lower than the equilibrium redox state in the experimental apparatus. After pre-treatment in the IHPV the Fe^{2+}/Fe_{tot} ratio increases from 0.41 (MDIB1, Table 1) to 0.61 (MDIB 12, Table 2). The latter value represents the lower limit of Fe^{2+}/Fe_{tot} adjustable in the IHPV. Hydrogen fugacity in the vessel is typically ~0.2 bar at intrinsic conditions, resulting in an oxygen fugacity close to that buffered by the MnO-Mn_3O_4 (MMO) assemblage if pure H_2O fluid is present in the capsule (Berndt et al., 2002).

To produce a strongly reduced water-poor glass, powder from MDIB2 glass was mixed with an appropriate portion of carbon, filled into a graphite crucible, and melted for 1 h at 1523 K in an oven flushed with a gas mixture composed of 93% Ar and 7% H_2. The obtained sample had a very high average Fe^{2+}/Fe_{tot} ratio of 0.91 (sample R13 in Table 2) but visually appeared to be inhomogeneous. To improve homogeneity and to compact the samples, the glass was crushed, filled in a large AuPd capsule (diameter of 8mm), and re-melted for 30 min at 1573 K, 500 MPa under intrinsic conditions in the IHPV. The post-experimental analysis yielded a Fe^{2+}/Fe_{tot} ratio of 0.83 close to the initial value (Table 2).

The procedure to synthesize water-bearing glasses is described in detail by Vetere et al. (2006). Distilled water was added stepwise to a dry glass powder in AuPd capsules (diameter of 5-6 mm, length of 30-40 mm). Relatively oxidized glasses (MDIB32, MDIB30, MDIB29 MDIB25, MDIB24, MDIB12 MDIB10, MDIB4, J1) were produced by annealing at 300-500 MPa and 1523 K for 24 h under intrinsic conditions of the IHPV. To synthesize hydrous glasses with high Fe^{2+}/Fe_{tot} (R6, R7, R9, R10), runs were performed for 20 to 70 h at 1323 K and 200 MPa in an IHPV at an elevated hydrogen pressure. In these runs the amount of H_2O (10 wt% relative to the loaded glass powder) in the capsule was in excess to the expected water solubility and Au capsules were used which are more efficient than AuPd capsules to depress iron loss. Hydrogen fugacity was monitored with a Shaw membrane as described in Berndt et al. (2002). In the syntheses of samples R6 and R7 the hydrogen fugacity was at f_{H2} = 6.4 bar while more reducing conditions of f_{H2} = 20 bar were adjusted for R9 and R10 (see Table 2).

Samples were quenched either by the rapid quench method (see Berndt et al. 2002) or by normal quench (by switching off the power; initial cooling rate is about 200 K / min). Using the rapid quench method avoids the formation of quench crystals, but the glass cylinders

accumulate stress and often brake. In such a case, the cylinders can not be used for a second viscosity determination. On the other hand, the normal quench method allows multiple experiments with the same glass, but quench crystals are formed. To check whether quench crystals could influence the viscosity measurements, we performed annealing experiments in which a quench crystals-bearing sample was heated up and quenched (using the rapid quench technique) immediately after reaching the target temperature. After such treatments at 1423 K and at 1473 K the quench crystals dissolved completely. Hence, we do not expect any influence of quench crystals on the viscosity experiments.

For the viscosity experiments a cylinder (diameter: 4 or 5 mm; length: 10 – 15 mm) was cored out of the synthesized glasses. The residual glass was crushed to fine grained powder except for some fragments to be used for determination of the water content and the Fe^{2+}/Fe_{tot} ratio. Loading procedure of capsules for viscosity experiments is described in detail by Vetere et al. (2006).

2.2. Electron microprobe analyses

The chemical composition of the glasses was determined by electron microprobe Cameca SX100. Measurement conditions were: defocused beam of 15 µm diameter, accelerating voltage of 15 kV and a beam current of 4 nA. The nominally dry andesitic glasses MDIB1 and MBIB2 are more mafic than those used by Liebske et al. (2003) and Neuville et al. (1993) (see Table 1). Silica content was slightly higher in hydrous viscosity samples (average value for six samples is given as MDIBvis in Table 1) than in the dry starting glasses. We attribute these deviations to inhomogeneities in the starting glass. The average composition MDIBvis is considered to be representative for our viscosity samples. Consistency of the

overall dataset implies that slight variations in compositions (except for water content and Fe^{2+}/Fe_{tot}) have minor influence on viscosity.

2.3. Water determination

The water content of the glasses was determined by Karl-Fischer Titration (KFT) and infrared spectroscopy (IR). To account for unextracted water (Behrens and Stuke, 2003), water contents measured by KFT were corrected by adding 0.13 wt% H_2O. The accuracy of the KFT analysis is estimated to be 0.10 wt%, including the uncertainty in the amount of unextracted water and the error in the titration rate (for details of the analytical technique and error estimation see Behrens and Stuke, 2003 and Leschik et al., 2004). To test the homogeneity of H_2O concentrations in selected samples, wafers from different part of the samples were analyzed by KFT. Data are labelled with the superscript *t* (top), *b* (bottom) and *c* (center) in Table 2. Variation of water content was always within the analytical error.

Mid-infrared (MIR) absorption spectroscopy was used to characterize the water content of water-poor glasses. Absorption spectra of doubly polished glass slabs with thickness of 0.05-0.30 mm were recorded using an IR microscope Bruker IRscopeII connected to an FTIR spectrometer Bruker IFS88. Water contents were derived from the peak height of the OH stretching vibration band at 3550 cm^{-1} after subtraction of a linear baseline. The absorption coefficient of 62.3 L $mol^{-1}cm^{-1}$ determined by Mandeville et al. (2002) was used in the evaluation of the MIR spectra.

Water distribution in some water-rich post-experimental glasses was measured using near-infrared (NIR) spectroscopy. Simple linear baselines were fitted to the OH combination band at 4500 cm^{-1} and the molecular H_2O band at 5200 cm^{-1} (TT baseline according to Ohlhorst et

al., 2001). This baseline correction is reliable to quantify the total water content but may have systematic errors in the determination of hydrous species concentrations (cf Ohlhorst et al., 2001). However, water speciation measured in glasses at room temperature does not reflect the equilibrium speciation in the melt during viscosity experiments (Dingwell and Webb, 1990), and, hence, it is not important for the interpretation of our viscosity data.

2.4. Colorimetric determination of ferrous iron in silicate glasses

A 6 mg to 9 mg portion (glass chips) of each sample was used for determination of ferrous-ferric ratios using a colorimetric method modified after Wilson (1960). Samples were dissolved with concentrated HF to which a solution of ammonium vanadate in 5 M sulfuric acid was added. At these acid conditions the released ferrous iron reacts with V^{5+} forming V^{4+} and ferric iron (reaction $Fe^{2+} + V^{5+} = Fe^{3+} + V^{4+}$). The reaction products are more stable with respect to oxidation in air than ferrous iron so that the initial redox state of the glass is preserved in the solution. After complete sample dissolution at room temperature we added saturated hot boric acid (353 K) instead of beryllium sulfate as proposed by Wilson (1960) to neutralize excess HF and to bring eventually formed fluorides back into solution. Fe^{2+} is regenerated by adjusting a pH value of ~5 using an ammonium acetate buffer. For the colorimetric analysis 2:2'bipyridyl was added which forms a stable complex with Fe^{2+}. To quantify the concentration of this complex we have used the characteristic absorption band at 523 nm. Measurements of concentrations of ferrous Fe and total Fe were made on the same solution before and after adding solid hydroxylamine hydrochloride. This reducing agent converts all ferric Fe into the ferrous state. Since both Fe^{2+} and total Fe determination was done on the same solution, uncertainties in the Fe^{2+}/Fe_{tot} ratios arise mainly from the absorbance measurements for which a 1 cm transmission cell in an UV/VIS spectrometer

Zeiss Specord S10 was used. Calibration of the spectrometric technique was made by measuring ferrous ammonium sulfate solutions with different known Fe^{2+} concentrations.

In each analytical session several internal standards were processed to assess the accuracy and reproducibility of the method. These standards included the glassy USGS standard RGM-1 rhyolite, and two synthetic glass in-house standards, PU-3 andesite and CT-1 basalt (synthesized from oxides and carbonates at 1873 K in air). The mean values of Fe^{2+}/Fe_{tot} (all ± 2σ error) determined by the colorimetric method are 0.77 ± 0.04 for RGM-1 (n=11), 0.38 ± 0.03 (n=25) for PU-3, and 0.41 ± 0.02 (n=8) for CT-1. For RGM-1 the determined values of ferrous Fe (FeO = 1.31 ± 0.06 wt%) and total Fe (FeO_{tot} = 1.69 ± 0.04 wt%) are equivalent within the given 1σ errors with the certified values (FeO = 1.27 ± 0.05 wt%; FeO_{tot} = 1.67 ± 0.03 wt%; Fe^{2+}/Fe_{tot} = 0.76 ± 0.03). The total Fe concentrations of the synthetic glass standards determined with the colorimetric method (PU-3 FeO_{tot} = 7.57 ± 0.06 wt%; CT-1 FeO_{tot} = 12.93 ± 0.70 wt%) are in good agreement with FeO_{tot} analyses by electron microprobe (PU-3 FeO_{tot} = 7.74 ± 0.42 wt%; CT-1 FeO_{tot} = 13.17 ± 0.47 wt%). From the results of the replicate analyses of different standards, the precision assigned to the reported Fe^{2+}/Fe_{tot} ratios is ± 0.03 (2σ).

The Fe^{2+}/Fe_{tot} ratios of glasses before viscosity experiments and after viscosity experiments are given in Tables 1 and 2. No significant change in redox state is observed during the viscosity determination **(Fig. 1)**. Comparison of the Fe^{2+}/Fe_{tot} ratio of the air-melted starting material (Table 1) with those of the viscosity samples (Table 2) emphasize the importance of pre-equilibration of samples at similar conditions as used in the viscosity experiments. Fe^{2+}/Fe_{tot} ratio of air-melted glasses are in the range of 0.41 – 0.44 whereas samples processed in the IHPV have redox ratios above 0.58.

2.5. Falling sphere experiments

Determination of viscosity required the measurement of the exact position of the sphere in the glass cylinder before and after experiment. A thin layer of Pt powder was inserted in the viscosity samples as internal reference for distance measurements. Due to small grain size (~ 0.8 μm) the Pt powder is essential immobile during the experiment. Because the glasses are not transparent in the visible we have used X-ray images to monitor sphere positions (SIEMENS HELIODENT DS X-rays camera with voltage of 60 kV and anode current of 7 mA, KODAK INSIGHT IP-21 films, and exposure time of 0.16 s). Some run products were cracked and could not be completely expelled from the capsule without destruction. In this case only part of the capsule was removed to enable recording X-ray images. To calibrate the images, we have used a transparent glass piece with copper wires in well defined intervals (**Fig. 2**). The distance between the wires was measured on a microscope stage equipped with a micrometer scale. In some experiments, we used more than one sphere (Pt and Pd spheres) that allowed us multiple determination of viscosity.

After welding shut the capsule, a pre-experiment was performed in an IHPV for a few minutes to establish well-defined starting positions of the spheres with respect to the Pt powder layer (condition: 1523 K and 300-500 MPa for AuPd capsules; 1323 K and 200 MPa for Au capsules). The pre-experiment gave a raw estimate for the melt viscosity. However, due to initial compaction of the sample and thus due to a poorly constrained starting position of the sphere, this measurement is less precise than the subsequent runs and it is not included in Table 2. Up to four viscosity determinations were carried out with the same sample. A long

total descent distance could be achieved by turning the sample upside down when the sphere approaches the platinum layer.

Most of the viscosity experiments were performed under intrinsic conditions in IHPV as described in Vetere et al. (2006). Samples R6, R7, R9 and R10 were processed at same hydrogen fugacity as used for the glass syntheses. Run duration was always short (300 – 3000 s) so that only minor changes in iron content or redox state of iron were expected during the viscosity experiments.

Some additional experiments at elevated pressures of 1000 – 2000 MPa were performed in an end-load ¾ inch piston cylinder apparatus, PCA, (Voggenreiter company) at INGV in Rome. We have used a NaCl-crushable alumina-pyrex assemblage for the nominally dry sample MDIB12 and a crushable alumina-pyrophyllite-pyrex assemblage for the hydrous samples MDIB24 and MDIB25 (see Freda et al. (2001) for the effect of assemblage on water budget of capsules processed in PCA). Experiments were first pressurized and then heated at a rate of 200 K/min up to 20 K below the target temperature. A smaller rate of 40 K/min was applied within the last 20 K of heating to avoid overshooting. Temperature was controlled within ±3 K using one $W_{95}Re_5$-$W_{74}Re_{26}$ (type C) thermocouple located on top of the sample. The experiment was terminated by switching off the heating power while maintaining pressure constant. The initial quench rate was about 2000 K/min.

The viscosity η is calculated by Stokes law

$$\eta = \frac{2 \cdot t \cdot g \cdot \Delta\rho \cdot r^2 \cdot C_F}{9 \cdot d} \qquad (1)$$

where d is the settling distance in cm, t is the run duration in sec, $\Delta\rho$ is the density difference between the sphere and the melt, g is the acceleration due to gravity (9.81 m/s^2), r is the radius of the sphere and C_F is the Faxen correction (Faxen, 1923) to account for the effect of viscous drag by the capsule wall on the settling sphere. To account for movement of spheres during heating and cooling, we calculated the effective run duration for each experiment as described in Vetere et al. (2006). Room temperature densities of Pt and Pd are 21.45 and 12.02 g/cm^3, respectively. No correction was made for differential compression and thermal expansion of the solid materials because this would contribute less than 1% to the viscosity. The density of hydrous andesitic glasses as a function of the total water content, C_{H_2O} (in wt %) was calculated with the equation

$$\rho = 2661\,(\pm 7) - 18.4\,(\pm 2.0)\cdot C_{H_2O} \qquad (2)$$

reported by Ohlhorst et al. (2001). When the melt density at experimental conditions is used in Eqn. 1 instead of the glass density, the viscosity is higher by at most 3% (Vetere et al., 2006). This difference is small compared to the experimental error of viscosity and we did not correct for it.

The settling distance was measured with Corel Draw 12 software after scanning the X-ray images with a resolution between 600 and 1200 dpi. The estimated error of distance measurement is about ± 10 µm, mainly determined by the resolution of the micrometer scale on the microscope stage. This error, together with the uncertainty in run duration, in radius of spheres and in temperature (estimated to be ± 30s, 1-5 µm and ± 10 K, respectively; see Vetere et al., 2006) accumulate to an overall error in viscosity determination of 9 - 14 % (Table 2). Viscosity values measured using spheres with different radii inserted in the same sample are identical within uncertainty for MDIB4, MDIB10a, MDIB29, MDIB30a and

MDIB30b (Table 2). However, larger deviations than expected from this error estimate were observed for samples MDIB32 and MDIB31. Possible explanation could be deformation of spheres induced by capsule loading and initial compression as observed for haplogranitic samples (Holtz et al. 1999). Thus in some cases the effective radius of the sphere may differ from that determined before experiment. Unfortunately, the iron-bearing glasses are not transparent and possible deformation of spheres could not be verified.

2.6. Creep experiments

Creep experiments under pressure were performed to measure melt viscosity above the glass transition temperature. Experimental procedures follow those described by Schulze et al. (1999). The rate of deformation of cylindrical glass samples is measured when applying a constant uniaxial stress (Neuville and Richet, 1991). The viscosity is calculated as:

$$\eta = \frac{\sigma}{3 \cdot \frac{d \ln l}{dt}} \qquad (3)$$

where σ is the applied stress and l is the length of the cylinder. The reproducibility of viscosity measurements with the high pressure parallel plate viscometer is within ± 0.15 log unit (Schulze et al., 1999). To check for possible water loss during creep experiments, polished sections along the cylindrical axis were prepared and analyzed by IR microspectroscopy.

In previous studies, rapid crystallization of iron oxide was a major problem in measurement of the viscosity of andesitic melts near the glass transition (Neuville et al., 1993; Richet et al., 1996; Liebske et al., 2003). In order to minimize the influence of crystallization, the samples were heated as fast as possible to the temperature of the first viscosity measurement. Hence, the viscosity data have higher uncertainty than in previous studies because the apparatus was

not completely relaxed, but the overall error of the viscosity data obtained from experiments is estimated to be within ± 0.2 log unit.

3. Results

3.1. Falling sphere experiments

The falling sphere data cover a range of water content from nominally dry to 6.2 wt%, of Fe^{2+}/Fe_{tot} from 0.61 to 0.83 (considering data after experiments) and of temperature from 1323 to1573 K (Table 2). The minimum viscosity measured with the falling sphere method is 4.9 Pa·s using a Pd sphere with a radius of 61 µm and 5 min run time at 1473 K (Table 2, sample MDIB32a). Runs at same temperature and pressure using samples with similar water content and redox state of iron agree within 0.17 log units (R6, R7) and 0.33 log units (R9, R10). The relatively large deviation in the second case is probably due to the uncertainty in run duration for the short experiment R9 (dwell time of only 420 s) but could be affected also by deformation of the sphere.

In the experiments it was not possible to vary Fe^{2+}/Fe_{tot} independent on water content because both properties are linked by the hydrogen fugacity imposed by the vessel. Hence, the influence of Fe^{2+}/Fe_{tot} on viscosity at given water content and temperature can be inferred only by considering trends in the whole dataset. The effect of redox state of iron appears to be very low for water-rich samples (2.5 to 6.2 wt% H_2O) in the Fe^{2+}/Fe_{tot} range of 0.61- 0.76. At 1323 K, the viscosity of samples R6, R7, R9 and - R10 (Table 2) containing 4.8 to 5.2 wt% H_2O varies only between 14 and 31 Pa·s for Fe^{2+}/Fe_{tot} ratios increasing from 0.62 to 0.77. No clear tendency (increasing or decreasing viscosity with changing Fe^{2+}/Fe_{tot}) is observed in the dataset. In contrast, in melts with low water contents, the viscosity decreases noticeably with

increasing Fe^{2+}/Fe_{tot} ratio. The comparison of data obtained for "nominally dry" samples (e.g. R13 and J1; Table 2) in the high temperature range indicate that changing Fe^{2+}/Fe_{tot} from 0.83 to 0.60 may cause a variation of up to 1 log unit. Although there is a difference of 50 K between experiment R13 and J1, it is obvious that the viscosity is higher in the melt with the lowest ratio Fe^{2+}/Fe_{tot}.

3.2. Creep experiments

Creep experiments were successful only with one sample containing 3.3 wt% H_2O (MDIB7, Table 3). An attempt with a sample containing 5.1 wt% H_2O failed due to rapid loss of water during viscosity measurement. The viscosity datum obtained for this glass at 792 K was about 1 log unit higher than that predicted by our new model (see below) and by the variation of viscosity with water content observed for iron-free analogue compositions (Richet et al. 1996; Vetere et al. 2006). The sample shows a dehydrated rim after experiment which probably has strongly strengthened the sample.

With the sample MDIB7 three measurements at the same temperature (747 K) were performed during the experimental sequence (**Fig. 3**). The obtained viscosity data agree within ±0.15 log units. However, the viscosity-time record shows an increase of viscosity with time already for the second measurement, indicating that iron-oxides started to crystallize from the glass (Richet et al. 1996; Liebske et al. 2003). But the change in viscosity is small and we suggest that the data presented in Table 3 are still representative for the andesitic melts. Water determination by KFT after the experiments agree within the value measured for the starting glass, indicating that water loss was not severe during the experimental sequence with MDIB7.

4. Discussion

4.1. Loss of iron during experiments and implication for viscosity determination

One problem with high pressure experiments using Fe-bearing samples at high temperature is the loss of iron from the melt to the capsule material, in particular at low water content of the melt and high hydrogen fugacity in the vessel (e.g., Sisson and Grove, 1993; Berndt et al., 2005). The loss of iron was quantified using the colorimetric method and/or electron microprobe. For the centre of the glass cylinders electron microprobe analysis yielded similar iron content when compared with bulk measurements using colorimetry (Table 4). Near the capsule walls (see **Fig 4**) the melts were more depleted in iron content, but this may not have affected the viscosity data because the spheres are located close to the cylindrical axis of the sample.

Experiments performed in Au capsules (Table 2) show only little changes in iron contents when compared to the starting material despite of high hydrogen fugacity in the IHPV, in agreement with studies on basaltic system using the same IHPV (Berndt et al., 2005). The iron loss for samples R6 to R10, with starting material MDIB2 (Table 1) is 0.5 ± 0.3wt% FeO_{tot}. The iron loss is more significant when using AuPd capsules, even at low hydrogen fugacity (intrinsic conditions of IHPV). Among the samples analyzed for iron loss, two glasses (MDIB30, MDIB25) are products from experiments conducted at the highest temperature (1523 K). One of these samples (MDIB30) was even used in a series of experiments at different temperatures. Thus, the iron loss is expected to be particularly strong for this sample. However, the loss of 1.7 wt% FeO_{tot} detected for MDIB30 is similar to the value found for MDIB25 (2 wt% FeO_{tot}). Glasses from experiments performed at 1473 K show similar or slightly lower iron loss (MDIB31 and MDIB32). Thus, iron loss is low but

not negligible in our experiments performed in AuPd capsules. The problems related to iron loss may explain some differences in viscosity obtained at similar conditions (water content and temperature). For example, the viscosity determined in experiment MDIB32d (1323 K, 6.2 wt% H_2O), in which 2 wt% FeO_{tot} loss was observed, is higher than the viscosity determined in experiment R6 (1323 K, 5.2 wt% H_2O) with less than 0.7 wt% FeO_{tot} loss (compare Table 2). Since the water content in MDIB32d is higher than in R6, a lower viscosity is expected from the experiment MDIB32d.

4.2. Viscosity model for Fe-bearing andesite melt

The originality of our dataset is that it allows us to improve the viscosity model for andesite melt established for a Fe-free composition by Richet et al., (1996) and Vetere et al. (2006). These authors showed that the effect of dissolved water on andesitic melts is more pronounced at low than at high water content, as expected from other compositions investigated in the past (e.g., Hess and Dingwell, 1996; Richet et al., 1996; Scaillet et al., 1996; Schulze et al., 1996, 1999; Romano et al., 2001, 2003; Whittington et al., 2000, 2001; Liebske et al., 2003; Zhang et al., 2003; Giordano et al., 2004a,b). Several studies (Mysen and Virgo 1989, Dingwell and Virgo 1988, Dingwell 1991, Liebske et al., 2003) have shown that oxidation state of iron is a parameter which needs to be taken into account to model the viscosity of silicate melts with high Fe contents. In the system Na-Si-Fe-O (composition NS4F40) and at 1473 K, Dingwell and Virgo (1988) observed a decrease in viscosity by 0.81 log units when increasing the Fe^{2+}/Fe_{tot} ratio from 0 to 0.77. Moreover a decrease in log viscosity of 0.34 log units was found for $NaFeSi_2O_6$ melt when increasing the Fe^{2+}/Fe_{tot} ratio from 0.08 to 0.82 at 1703 K. As shown in Liebske et al. (2003), when the Fe^{2+}/Fe_{tot} ratio increases from 0.42 to 0.79 in an andesite melt, the viscosity decreases by ~1.7 log units at

1061 K. This indicates that previous determinations made at ambient conditions (high oxygen fugacity) may not be geologically relevant.

A major problem in setting up a viscosity model for andesite melts is due to inconsistencies within and between the data sets published for viscosity of andesitic melts and due to the lack of information on the redox state of iron in most of previous studies. In the high viscosity range (just above the glass transition) published data for nominally dry andesitic melts cover a range of more than two orders of magnitude at constant temperature (see data compilation in Liebske et al. (2003), Fig. 10). In part these viscosity variations may be due to variations in melt composition and/or differences in redox state of iron. Liebske et al. (2003) found a decrease in viscosity by 1.7 log units in average when Fe^{2+}/Fe_{tot} increases from 0.42 to 0.79. Additionally, differences in the applied experimental techniques and bulk composition may contribute to the variation in viscosity data for dry andesite (Goto et al., 1997, and Taniguchi, 1993, used fiber elongation; Neuville et al., 1993, and Richet et al., 1996, performed creep experiments at 1 atm; Liebske et al., 2003 used high pressure parallel plate viscometry). However, a severe problem in the low temperature studies is also rapid crystallization of iron oxides, especially in oxidized melts (Neuville and Richet, 1991; Richet et al., 1996; Liebske et al., 2003). Hence, actual experimental data are often difficult to interpret in terms of the viscosity of a supercooled crystal-free andesitic melt.

In our modelling we consider for water-poor melts in the high viscosity range only data from Liebske et al. (2003) because of the unknown redox state of iron (and possible effect of crystallization of iron oxides) in the other studies (Taniguchi, 1993; Goto et al., 1997; Neuville et al., 1993; Richet et al., 1996). Data for the viscosity of hydrous melts near the glass transition are limited to one measurement on a sample containing 1.88 wt% H_2O

studied by Liebske et al. (2003) and five measurements on a sample containing 3.30 wt% H_2O measured in this study (Table 3, sample MDIB 7). Redox state of iron is similar in both melts and, hence, variation of viscosity with Fe^{2+}/Fe_{tot} can not be constrained for hydrous melts in the high viscosity range. However, minor variation of η with Fe^{2+}/Fe_{tot} were observed for dry melts with similar Fe^{2+}/Fe_{tot} (0.70) at high viscosity and the viscosity of water-rich melts above the liquidus is not sensitive to Fe^{2+}/Fe_{tot}. Thus we infer that the data for hydrous samples just above the glass transition can be applied in a wider range of Fe^{2+}/Fe_{tot} without significant error (between 0.65 and 0.75).

Although several data sets are available for the viscosity of andesitic melts above the glass transition (Murase and McBirney, 1973; Kushiro et al., 1976; Persikov et al., 1990; Neuville et al., 1993; Goto et al., 1997), the data can not be used directly for modeling viscosity because of the unknown redox state of iron for these experiments. Data measured at ambient pressure using the concentric cylinder technique (Neuville et al., 1993) and the counter balanced sphere method (Murase and McBirney 1973; Goto et al., 1997) cover a narrow range in viscosity at given temperature, implying that small differences in compositions have minor effect on viscosity of andesite-like melts. For modeling we have estimated the redox state of iron in the melts using the model of Moretti (2005). Assuming equilibrium of the melt with the surrounding air, these redox calculations indicate very large changes in Fe^{2+}/Fe_{tot} with temperatures (from $Fe^{2+}/Fe_{tot} = 0.35$ at 1867 K to $Fe^{2+}/Fe_{tot} = 0.055$ at 1433 K). Unfortunately, it was not possible to design a simple model which describes well the data for very oxidized and for more reduced melts. Because we do not know reliably the redox state the melts in the superliquidus experiments we restricted ourselves to design a simple model applicable only to reduced melts ($Fe^{2+}/Fe_{tot} > 0.3$). However, andesitic melts in nature usually are not very oxidized, except may be for melts exposed to the earth surface. Thus we suggest

that our new model, even when being not applicable in air, it nevertheless has great potential for application to andesitic melts at geologically relevant conditions.

The data base for modelling the viscosity as a function of temperature, water content and Fe^{2+}/Fe_{tot} ratio consists of 46 measurements from Liebske et al. (2003) and 36 measurements from our new study. An empirical viscosity model based on the VFT approach was chosen to account for the non-Arrhenian temperature dependence of viscosity. Data were fitted using a non-linear least-square regression. After various attempts of trial and error the following equation was found best to reproduce the experimental data and the observed viscosity trends

$$\log \eta = -4.26 + \frac{5515.26}{(T - 275.43)} + \frac{1907.23}{(T - 626.24)} \cdot \exp\left[\frac{218.66}{\left(\frac{Fe^{2+}}{Fe_{tot}} \cdot T\right)}\right] * \exp\left(-469.1 \cdot \frac{w}{T}\right) \qquad (4)$$

where η is the viscosity in Pa·s, T the temperature in K, w is the water content in wt% and Fe^{2+}/Fe_{tot} is the relative proportion of ferrous iron. This equation reproduces the experimental data with a 1σ standard deviation of 0.17 log units (**Fig. 5**). The predicted trends for different redox ratios of iron are plotted in **Fig. 6**. For water-rich melts difference due to Fe^{2+}/Fe_{tot} can not be resolved by the experimental data. It has to be emphasized that the dependence on redox ratio of iron is constrained mainly by the data for dry melts at low temperature (Liebske et al. 2003) and our high temperature data (samples MDIB12, R13).

Noteworthy, the new empirical model is constrained only for $Fe^{2+}/Fe_{tot} > 0.3$. More oxidized melts show discrepancies to the model in particular at low temperatures. At temperatures around 1800 K Eqn. (4) agrees well with measurements using the concentric cylinder

technique and counter balanced sphere method in air (Neuville et al., 1993; Murase and McBirney, 1973; Goto et al., 1997) when estimating the redox state of iron after Moretti (2005). However, already at 1700 K the model overestimates the viscosity by one order of magnitude, and the difference is strongly growing with decreasing temperature. Furthermore, as noted above, the variation of viscosity with water content is uncertain because only few experimental data are available. The predictions have to be verified by additional experiments with water-bearing melts in the low temperature range. Finally, it has to be emphasized that the model is not applicable at temperatures below the glass transition.

The viscosity model of Vetere et al. (2006) determined for a Fe-free andesite is compared with the predictions of Eqn. (4) to check the applicability of viscosity models elaborated for Fe-free melts. **Fig. 7** shows the effect of water on viscosity of Fe-free and Fe-bearing andesitic melts with Fe^{2+}/Fe_{tot} of 0.7 at 1273 and 1473 K. This Fe^{2+}/Fe_{tot} ratio is representative for a f_{O2} corresponding approximately to the QFM buffer at high temperature, which is relevant for geological conditions in magma chambers. Significant differences (up to approximately 1 order of magnitude) between the two models are observed at low water contents. The differences become less pronounced at water contents higher than 4 wt% H_2O. Differences become larger at low temperature but melts with an andesitic composition partially crystallize at 1273 K and water contents below 4 wt% (e.g., Botcharnikov et al., this issue).

4.3. Pressure effect on viscosity of andesitic melts.

Scarfe et al. (1987) found in the low viscosity range that in some silicate melts with NBO/T>1, like $CaMgSi_2O_6$, viscosity increases with pressure, whereas most silicate and aluminosilicate melts with NBO/T<1 $NaAlSi_3O_8$, $NaAlSi_2O_6$, K_2O-MgO-5 SiO_2, andesite,

tholeiitic basalt, are characterized by a negative pressure effect (decrease in viscosity with increasing pressure). An "anomalous" negative pressure effect on viscosity was found also in the high viscosity range for polymerized melts such as albite melts or tonalite melts (Schulze et al., 1999; Behrens and Schulze, 2003). In the system albite-diopside a crossover between positive and negative pressure dependence of viscosity was found between an NBO/T of 0.1 to 0.3 (composition close to $Ab_{74}Di_{26}$), depending on temperature (Behrens and Schulze 2003). From these studies a minor effect of pressure on melt viscosity is expected for andesitic melts. Results from Liebske et al. (2003) confirm this suggestion in the high viscosity range (10^{8}-$10^{11.5}$ Pa s) for Fe-free andesitic analogue composition with water contents from 0 to 2 wt%. In the pressure range from 0.1 to 300 MPa the variation of viscosity was found to be less than 0.3 orders of magnitude. In the low viscosity range, Vetere et al (2006) found no significant dependence of viscosity on pressure in the range 0.1 to 500 MPa for a melt with similar composition. Thus, in Fe-free andesites, the effect of pressure is minor and can be neglected for geologically relevant conditions.

Results of falling sphere experiments with Fe-bearing andesite melts in the pressure range from 200 to 2000 MPa suggest that pressure is of minor influence for andesitic melts at geological relevant conditions. The overall consistency of the data and the agreement between modelled and experimental data (**Fig. 5**) support this conclusion, although we do not have experimental pairs in which only pressure is changing (identical water content, Fe^{2+}/Fe_{tot} and temperature).

5. Implication for mixing-mingling processes at Unzen volcano

It has been emphasized in previous studies (e.g., Nakada and Motomura, 1999; Venezky and Rutherford, 1999; Holtz et al., 2005) that the Unzen dacite of the 1991-1995 eruption was probably generated from a mixing process between a phenocryst-rich low-temperature (rhyolitic) and a nearly aphyric high-temperaure magma (basalt-andesitic). This is based on petrographic observations with plagioclase and hornblende phenocrysts showing compositional zoning and reverse zoning at the rims (Nakamura, 1995; Nakada and Motomura, 1999) and on experimental phase equilibria investigations (Venezky and Rutherford, 1999; Holtz et al., 2005; Sato et al., 2005; Botcharnikov et al., 2006). It has been proposed that mixing of an almost aphyric high temperature andesitic magma with a phenocryst-rich low temperature rhyolitic magma has initiated the 1991 eruption of the Unzen volcano (Nakada and Motomura, 1999 Venezky and Rutherford, 1999). The andesitic composition of the high temperature end-member has been recently questioned by Browne et al. (2006), suggesting that it may have been basaltic on the basis of the analysis of mafic enclaves from the historical Unzen volcanic sequence. However, since no mafic enclave with a basaltic composition has been found in the products of the 1991-1995 eruption, the following discussion is based on previous models, assuming an andesitic end-member. In this hypothesis, the temperature of the injected andesitic magma is estimated to be near 1323 K with a water content of 4 wt% (Holtz et al., 2005; Sato et al., 2005). The temperature of the partially crystallized magma in the chamber before mixing is estimated to be 1033 – 1053 K and the water content of the residual rhyolitic melt is inferred to be about 8 wt% (Holtz et al., 2005).

Among the parameters governing the efficiency of mixing processes, viscosity is a crucial factor. Using viscosity models elaborated for hydrous rhyolitic melts (Hess and Dingwell, 1996) and for Fe-bearing andesitic melt (this study) the melt viscosities prior to eruption, the evolution of viscosities of mixed silicate melts and the efficiency of magma mixing at local scale can be estimated. **Figure 8a** shows the viscosity of the two end-member melts as a function of water content. Assuming a water content of 4 and 8 wt% H_2O for the andesitic and the rhyolitic melt, respectively, the melt viscosity is 50 Pa·s and $1.3 \cdot 10^4$ Pa·s, respectively, prior to eruption. Thus, directly after injection, the viscosity of the hot andesitic melt is about two orders of magnitude lower than that of the cold rhyolitic melt (Fig. 8a) and mingling processes, rather than mixing, between the two magmas should occur.

The average temperature of the magma after mixing is estimated to be 1173 to 1203 K (Venezky and Rutherford, 1999; Holtz et al., 2005). Assuming that equilibrium temperature is reached within a short period (mingling enhances equilibrium temperature distribution), the viscosity of the two end-member melts will change. Since thermal equilibrium is attained faster than chemical equilibrium in mingling/mixing processes, an important parameter governing efficient mixing (chemical homogeneity) at a local scale is the viscosity of melts which are reacting. Assuming a temperature of 1203 K (T after mingling/mixing), the andesitic melt with 4 wt% H_2O and Fe^{2+}/Fe_{tot} ratio of 0.65, would have a similar viscosity as the rhyolitic melt with 8 wt% (**Fig. 8b**). Assuming equilibrium conditions, the andesitic melt containing 4 wt% H_2O should crystallize at 1203 K and mixing processes will involve residual melts from a partially crystallized andesitic system and rhyolitic melts. However, at 1203 K, the viscosity of mixed melts (with a composition corresponding to the rhyodacitic groundmass) with water contents in between the two end-members (4 to 8 wt% H_2O) is not expected to differ strongly from that of the two end-members (increasing silica content is

compensated by the increasing water content). In conclusion, the nearly identical viscosity of the end members (independently on mixing ratios) and the low viscosity of the melts (10^3 Pa·s) favour chemical mixing processes. This is probably an important factor explaining the chemically homogeneous composition of the groundmass of Unzen dacite erupted over a period of 4 years.

Acknowledgements. This research was supported by the German Science Foundation (DFG grants Be1720/12. The authors thank the Japanese organisers of the Unzen Scientific Drilling Project, in particular S. Nakada, for the support of our work.

References

Behrens, H., Schulze, F., 2003. Pressure dependence of melt viscosity in the system $NaAlSi_3O_8$-$CaMgSi_2O_6$. Am. Mineral. 88, 1351-1363.

Behrens, H., Stuke, A., 2003. Quantification of H_2O contents in silicate glasses using IR spectroscopy - a calibration based on hydrous glasses analyzed by Karl-Fischer titration. Glass Sci. Tech., 76, 176-189.

Berndt, J., Liebske, C., Holtz, F., Freise, M., Nowak, M., Ziegenbein, D., Hurkuck, W., Koepke J., 2002. A combined rapid-quench and H_2-membrane setup for internally heated pressure vessels: description and application for water solubility in basaltic melts. Am. Mineral. 87, 1717-1726.

Berndt, J., Koepke, J., Holtz, F., 2005. An experimental investigation of the influence of water and oxygen fugacity on the differentiation of MORB at 200 MPa. J. Petrol. 46, 135-167.

Botcharnikov, R., Holtz, F., Almeev, R., Sato, H., Behrens, H., 2006. Storage condition and

evolution of andesitic magma prior to eruption of Unzen volcano: constrain from natural samples and experiments. J. Volc. Geothem. Res., this issue.

Bottinga, Y., Weill, D.F., 1972. Viscosity of Magmatic Silicate Liquids - Model for Calculation. Am. J. Sci. 272, 438-475.

Bouhifd, M.A., Richet, P., Besson, P., Roskosz, M., Ingrin, J. , 2004. Redox state, microstructure and viscosity of a partially crystallized basalt melt. Earth Planet. Sci. Lett. 218, 31-44.

Browne, B., Eichelberger, J.C., Patino, L.C., Vogel, T.A., Dehn, J., Uto, K., Hoshizumi, H. (2006) Generation of porphyritic and equigranular mafic enclaves during magma recharge events at Unzen volcano, Japan. J. Petrol., 47, 301-328.

Chen, H.C., De Paolo, D.J., Nakada, S., Shieh, Y.M., 1993. Relationship between eruption volume and neodymic isotopic composition at Unzen volcano. Nature, 362, 831-834.

Dingwell, D.B., Virgo, D., 1988. Viscosity oxidation state relationship for hedenbergitic melt. Carnegie Inst. Wash. Yearbook, 87, 48-53.

Dingwell, D.B., 1991. Redox viscometry of some Fe-bearing silicate melts. Am. Mineral. 76, 1560-1562.

Dingwell, D. B., Webb, S. L., 1990. Relaxation in silicate melts. Eur. J. Mineral. 2, 427-449.

Faxen, H., 1923. Die Bewegung einer starren Kugel längs der Achse eines mit zäher Flüssigkeit gefüllten Rohres. Ark. Math., Astro. Fysik, 17, 1-28 (in German).

Freda, C., Baker, D.R., Ottolini, L., 2001. Reduction of water loss from gold-palladium capsules during piston-cylinder experiments by use of pyrophyllite powder. Am. Mineral. 86, 234-237.

Giordano, D., Dingwell, D.B., 2003. Non-Arrhenian multicomponent melt viscosity: a model. Earth Planet. Sci. Lett. 208, 337-349.

Giordano, D., Romano, C., Dingwell, D.B., Poe, B., Behrens, H., 2004a. The combined

effects of water and fluorine on the viscosity of silicic magmas. Geochim. Cosmochim. Acta, 68, 5159-5168.

Giordano, D., Romano, C., Papale, P., Dingwell, D.B., 2004b. The viscosity of trachytes, and comparison with basalts, phonolites, and rhyolites. Chem. Geol. 213, 49-61.

Goto, A., Maedea, I., Nishida, Y., ,Oshima, H., 1997. Viscosity equation for magmatic silicate melts over a wide temperature range. Proc. Unzen Intern. Workshop: Decade volcano and scientific drilling. Shimabara, Japan. 100-105.

Grove, T.L., Elkins-Tanton, L.T., Parman, S.W., Chatterjee, N. Müntener, O., Gaetani, G.A., 2003. Fractional crystallization and mantle-melting controls on calc-alkaline differentiation trends. Contrib. Mineral. Petrol. 145, 515-533.

Hess, K.U., Dingwell, D.B., 1996. Viscosities of hydrous leucogranitic melts: A non-Arrhenian model. Am. Mineral. 81, 1297-1300.

Holtz, F., Roux, J., Ohlhorst, S., Behrens, H., Schulze, F., 1999. The effects of silica and water on the viscosity of hydrous quartzofeldspathic melts. Am. Mineral. 84, 27-36.

Holtz, F., Sato, H., Lewis, J., Behrens, H., Nakada, S., 2005. Experimental petrology of the 1991-1995 Unzen dacite, Japan. Part I: phase relations, phase chemistry and pre-eruptive conditions. J. Petrol. 46, 339-354.

Kushiro, I., Yoder, H.S., Mysen, B.O., 1976. Viscosities of basalt and andesite melts at high pressures. J. Geophys. Res. 81, 6351-6356.

Lejeune, A.M., Bottinga, Y., Trull, T.W., Richet, P., 1999. Rheology of bubble-bearing magmas. Earth Planet. Sci. Lett. 166, 71-84.

Lejeune, A.M., Richet, P., 1995. Rheology of crystal-bearing silicate melts - an experimental study at high viscosities. J. Geophys. Res.-Solid Earth, 100, 4215-4229.

Leschik, M., Heide, G., Frischat, G.-H., Behrens, H., Wiedenbeck, M., Wagner, N., Heide, K., Geißler, H., Reinholz, U., 2004. Determination of H_2O and D_2O contents in rhyolitic

glasses using KFT, NRA, EGA, IR spectroscopy, and SIMS. Phys. Chem. Glasses 45, 238-251.

Liebske, C., Behrens, H., Holtz, F., Lange, R.A., 2003. The influence of pressure and composition on the viscosity of andesitic melts. Geochim. Cosmochim. Acta 67, 473-485.

Mandeville, C.W., Webster, J.D., Rutherford, M.J., Taylor, B.E., Timbal, A., Faure K., 2002. Determination of molar absorptivities for infrared absorption bands of H_2O in andesitic glasses. American Mineralogist, 87(7): 813-821.

Moretti, R., 2005. Polymerization, basicity, oxidation state and their role in ionic modeling of silicate melts. Annals Geoph., 48 N 4/5, 583-608.

Murase, T., McBirney, R., 1973. Properties of some common igneous rocks and their melts at high temperatures. Geol. Soc. America Bull. 84, 3563-3592.

Mysen, B.O., Virgo, D., 1989. Redox equilibria, structure and properties of Fe-bearing alumosilicate melts: relationship among temperature, composition and oxygen fugacity in the system Na_2O-Al_2O_3-SiO_2-Fe-O. Am. Mineral. 74, 58-76.

Nakada, S., Motomura, Y., 1999. Petrology of the 1991-1995 eruption at Unzen: effusion pulsation and groundmass crystallization. J. Volc. Geotherm. Res. 89, 173-196.

Nakamura, M., 1995. Continuous mixing of crystals mush and replenished magma in the ongoing Unzen eruption. Geology 23, 807-810.

Neuville, D.R., Richet, P., 1991. Viscosity and mixing in molten (Ca, Mg) pyroxenes and garnets. Geochim. Cosmochim. Acta, 55, 1011-1019.

Neuville, D.R., Courtial, P., Dingwell, D.B., Richet, P., 1993. Thermodynamic and rheological properties of rhyolite and andesite melts. Contrib. Mineral. Petrol 113, 572-581.

Ohlhorst, S., Behrens, H. and Holtz, F., 2001. Compositional dependence of molar

absorptivities of near-infrared OH- and H_2O bands in rhyolitic to basaltic glasses. Chem. Geol. 174, 5-20.

Persikov, E.S., 1991. The viscosity of magmatic liquids: Experiment, generalized patterns. A model for calculation and prediction. Applications. Adv. Phys. Chem., 9, 1-41.

Persikov, E.S., Zharikov, V.A. Bukhtiyarov, P.G., Pol'skoy, S.F., 1990. The effect of volatiles on the properties of magmatic melts. Eur. J. Mineral. 2, 621-642.

Richet, P., Lejeune, A.M., Holtz, F., Roux, J., 1996. Water and the viscosity of andesite melts. Chem. Geol. 128, 185-197.

Romano, C., Poe, B., Mincione, V., Hess, K.U., Dingwell, D.B., 2001. The viscosities of dry and hydrous $XAlSi_3O_8$ (X = Li, Na, K, $Ca_{0.5}$, $Mg_{0.5}$) melts. Chem. Geol., 174, 115-132.

Romano, C., Giordano D., Papale P., Mincione V., Dingwell D.B., Rosi, M., 2003. The dry and hydrous viscosities of alkaline melts from Vesuvius and Phlegrean Fields. Chem. Geol. 202 , 23-38.

Sato, H., Nakada, S., Fujii, T., Nahamura, M., Suzuki-kamata, K.,1999. Groundmass pargasite in the 1991-1995 dacite on Unzen volcano: phase stability experiments and volcanological implication. J. Volcan. Geotherm. Res.89, 197-212.

Sato, H., Holtz, F.,Behrens, H., Botcharnikov, R., Nakada, S., 2005. Experimental petrology of the 1991-1995 Unzen dacite. Part II: Cl/OH partitioning between horneblende an melt and its implications for the origin of oscillatory zoning of horneblende phenocrysts. J. Petrol. 46 , 339-354.

Sato, H., 2005. Viscosity measurements of subliquidus magmas:1707 basalt of Fuji volcano. J. Mineral. Petrol. Sci. 100, 133-142.

Scaillet, B., Holtz, F., Pichavant, M., Schmidt, M., 1996. Viscosity of Himalayan leucogranites: Implications for mechanisms of granitic magma ascent. J. Geophys.

Res.-Solid Earth, 101, 27691-27699.

Scarfe, C.M., Mysen, B.O., Virgo, D., 1987. Pressure dependence of the viscosity of silicate melts. In Mysen, B. O. (ed.) Magmatic processes: physicochemical principles. Spec. Publ. Geochem. Soc. 1, 504-511.

Schulze, F., Behrens, H., Holtz, F., Roux, J., Johannes, W., 1996. The influence of H_2O on the viscosity of a haplogranitic melt. Am. Mineral. 81, 1155-1165.

Schulze, F., Behrens, H., Hurkuck, W., 1999. Determination of the influence of pressure and dissolved water on the viscosity of highly viscous melts: Application of a new parallel-plate viscometer. Am. Mineral. 84, 1512-1520.

Shaw, H.R., 1972. Viscosities of Magmatic Silicate Liquids - Empirical Method of Prediction. Am. J. Sci. 272, 870-893.

Sisson, T. W., Grove, T. L., 1993. Experimental investigations of the role of H_2O in calc-alkaline differentiation and subduction zone magmatism. Contrib. Mineral. Petrol. 113, 143–166.

Taniguchi, H., 1993. On the volume dependence of viscosity of some magmatic melts. Min. and Petrol. 49, 13-25.

Vetere, F., Behrens, H., Holtz, F., Neuville, D., 2006. Viscosity of andesitic melts – new experimental data and a revised calculation model. Chem. Geol. 228, 233-245.

Venezky, D.Y., Rutherford, M.J., 1999. Petrology and Fe-Ti oxide reequilibration of the 1991 Mount Unzen mixed magma. J. Volcan. Geotherm. Res. 89, 213-230.

Whittington, A., Richet, P., Holtz, F., 2000. Water and the viscosity of depolymerized aluminosilicate melts. Geochim. Cosmochim. Acta, 64, 3725-3736.

Whittington, A., Richet, P., Linard, Y., Holtz, F., 2001. The viscosity of hydrous phonolites and trachytes. Chem. Geol. 174, 209-223.

Wilson, A. D., 1960. The micro-determination of ferrous iron in silicate minerals by a

volumetric and colorimetric method. Analyst 85, 823-827.

Zhang, Y., Xu, Z.J., Liu, Y., 2003. Viscosity of hydrous rhyolitic melts inferred from kinetic experiments, and a new viscosity model. Am. Mineral. 88, 1741-1752.

Figure caption

Fig. 1. Comparison of the Fe^{2+}/Fe_{tot} ratio in glasses before and after experiments.

Fig. 2. X-ray images showing platinum and palladium spheres in an andesitic glass (left). Distance is measured relative to the platinum powder. A glass slide with copper wires in defined distance is used to calibrate the positions on the image (right).

Fig. 3. Creep experiment on sample MDIB 7 containing 3.30 wt% H_2O. Note that the viscosity started to increase with time at constant temperature from the third temperature step.

Fig. 4. Electron microprobe analyses showing a profile through the diameter of the sample. Note the depletion in Fe near the capsule wall.

Fig. 5. Comparison of experimental viscosity data for iron-bearing andesitic melts with predictions of the new model (Eqn. 4). IHPV, PPV and PCA in the legend refer to internally heated pressure vessel, parallel plate viscometer and piston cylinder apparatus respectively. Data from Liebske et al., (2003), LO3.

Fig. 6. Effect of redox state of iron and water content on the viscosity of andesitic melts at 1473 K.

Fig. 7. Comparison between the predictions of the model for Fe-free melts from Vetere et al., (2006) and those from our new model for natural andesite at 1273 and 1473 K.

Significant differences (up to approximately 1 order of magnitude) between the two models are observed at low water contents. The differences become less pronounced at water contents higher than 4 wt% H_2O.

Fig. 8. Viscosity of rhyolitic and andesitic melts at conditions prior to eruption of the Unzen volcano. The figure on top **(a)** shows the initial viscosity of the melt in the magma chamber (rhyolite) and in the ascending melt (andesite). This situation favours mingling of the magmas. The figure on bottom **(b)** illustrates the situation after thermal equilibrium. Similarity of viscosity observed in this case favours magma mixing.

Table 1. Electron microprobe analysis and water content of the starting material and selected viscosity samples (wt%).

	MDIB1	MDIB2	MDIB24	MDIB25	MDIB30	MDIBvis	Liebske et al. (2003)
SiO_2	55.11 (0.44)	54.18 (0.60)	57.60 (0.40)	59.56 (0.50)	56.86 (0.50)	59.32 (0.71)	56.65 (0.41)
TiO_2	1.09 (0.05)	1.09 (0.07)	0.92 (0.05)	0.93 (0.05)	1.04 (0.04)	1.02 (0.05)	1.01 (0.04)
Al_2O_3	18.39 (0.36)	18.41 (0.19)	14.98 (0.21)	15.45 (0.25)	16.90 (0.17)	16.76 (0.31)	17.41 (0.15)
FeO [a])	9.16 (0.32)	9.52 (0.33)	7.56 (0.39)	7.14 (0.35)	7.55 (0.38)	7.66 (0.43)	8.16 (0.21)
MnO	0.08 (0.06)	0.09 (0.06)	0.00 (0.08)	0.06 (0.04)	0.04 (0.04)	0.04 (0.06)	0.13 (0.04)
MgO	2.88(0.17)	2.93 (0.09)	2.77 (0.10)	2.79 (0.11)	3.14 (0.12)	3.05 (0.14)	4.30 (0.07)
CaO	8.44 (0.25)	8.69 (0.32)	6.37 (0.20)	6.46 (0.24)	7.13 (0.18)	7.16 (0.27)	7.38 (0.11)
Na_2O	3.38 (0.25)	3.41 (0.29)	3.06 (0.21)	3.26 (0.22)	3.31 (0.13)	3.38 (0.08)	3.23 (0.15)
K_2O	1.41 (0.08)	1.42 (0.08)	1.57 (0.08)	1.61 (0.07)	1.56 (0.06)	1.62 (0.08)	1.56 (0.07)
Fe^{2+}/Fe_{tot}	0.41	0.44	[b])	[b])	[b])		-
H_2O (IR)	0.015	0.016			2.88	see Table 2	0.015
H_2O (KFT)			4.80	3.32	2.95-2.91		
Total	99.98	100.02	99.63	100.56	100.43	100	99.85

Notes. Numbers in parenthesis correspond to 1 σ standard deviation. Analyses of andesites studied by Liebske et al. (2003) are shown for comparison. MDIB24 MDIB25 MDIB30 are average compositions of three samples after viscosity runs. MDIBvis represents the average of post-experimental analyses of six viscosity samples (MDIB4, MDIB 12, MDIB 24, MDIB 25, MDIB 30, MDIB 31, MDIB 32) normalized to a total of 100 wt%. H_2O contents were measured by IR spectroscopy using the peak height of the absorption band at 3550 cm^{-1} and the calibration of Mandeville et al. (2002) and/or by Karl-Fischer titration.
[a]) Total iron is given as FeO; [b]) Fe^{2+}/Fe_{tot} before and after experiments is given in Table 2.

Table 2. Experimental conditions and results of viscosity experiments using the falling sphere method.

No.	H_2O initial (wt%)	H_2O final (wt%)	P (MPa)	T (K)	Sphere radius (µm)	C_f	Dwell time (s)	Effective time (s)	Falling distance (cm)	η (Pa·s)	Fe^{2+}/Fe_{tot} before experiments	Fe^{2+}/Fe_{tot} after experiments
MDIB32a	6.10[t]		500	1473	61.5 ± 1 (Pd)	0.98	300	346	0.517	4.9 ± 0.7	0.58	
	6.31[b]				54± 1 (Pd)				0.219	9.3 ± 1.1		
MDIB32b				1423	61.5 ± 1 (Pd)		900	943	0.818	9.0 ± 0.9		
					54± 1 (Pd)				0.432	12.8 ± 1.2		
MDIB32c				1373	61.5 ± 1 (Pd)		900	940	0.649	11.1 ± 1.0		
					54± 1 (Pd)				0.316	18.1 ± 1.7		
MDIB32d		6.20[t]		1323	54± 1 (Pd)	0.98	2700	2735	0.603	53.4 ± 5.0		0.61
MDIB24	5.17[t]/4.78[b]	4.80[c]	1000*	1473	48± 1 (Pd)	0.98	900	923	0.303	14.5 ± 1.4	0.66	0.70
MDIB 4	3.67[t]/3.64[b]		500	1523	56 ± 1 (Pd)	0.98	360	409	0.291	8.9 ± 1.0	0.73	
					50 ± 1 (Pt)				0.403	10.2 ± 1.1		0.69
MDIB31	3.50[t]/		500	1473	62 ± 1 (Pd)	0.98	600	646	0.292	17.2 ± 1.7	0.73	
	3.44[IR]	3.30[b]			55 ± 1 (Pd)				0.125	31.6 ± 3.1		0.70
MDIB 10a	3.46[b]		500	1473	52 ± 1 (Pt)	0.98	393	439	0.135	34.9 ± 3.7	-	
					62.5 ± 1 (Pd)	0.98			0.097	32.3 ± 3.4		
MDIB 10b		3.38[t]	500	1523	52 ± 1 (Pt)	0.90	420	469	0.309	15.2 ± 1.6		0.70
MDIB25	3.36[t]/3.30[b]	3.32[c]	1000*	1523	72.5 ± 2.5 (Pt)	0.95	300	325	0.436	16.2 ± 1.8	0.68	
					57.5 ± 1 (Pt)	0.98			0.278	16.7 ± 1.9		0.68
MDIB30a	2.91[b]		500	1473	82.5 ± 2.5 (Pt)	0.98	600	646	0.619	28.6 ± 2.7	0.65	
	2.88[t-IR]				52 ± 1 (Pt)	0.98			0.245	28.7 ± 2.9		
MDIB30b				1423	82.5 ± 2.5 (Pt)	0.98	1020	1063	0.510	56.5 ± 5.2		
					52 ± 1 (Pt)	0.98			0.201	55.3± 5.3		
MDIB30c				1523	52 ± 1 (Pt)	0.98	300	349	0.105	36.3 ± 4.1		
MDIB30d		2.95[t-IR]		1373	82.5 ± 2.5 (Pt)	0.98	3000	3040	0.867	96.3 ± 8.5		
					52 ± 1 (Pt)	0.98			0.397	83.5 ± 7.8		0.66
MDIB 29	2.47[t]		500	1473	60 ± 2.5 (Pt)	0.98	600	646	0.379	24.7 ± 2.4	0.75	
	2.52[b]	2.47[t]			47± 1 (Pt)	0.98			0.263	21.9 ± 2.2		0.76
MDIB 12a		0.06[t-IR]	500	1523	200 ± 5 (Pt)	0.93	2700	2749	1.231	349.5 ± 34.1		
MDIB 12b		0.08[b-IR]	2000*	1473	200 ± 5 (Pt)	0.93	2700	2746	0.525	801.7 ± 80.1		0.61

R13	-	0.02^{IR}	300	1573	90 ± 2.5Pt	0.96	1200	1251	0.596	67.2 ± 7.4	0.91	0.83
J1	-	0.07 ^{IR}	300	1523	440 ± 5 Pt	0.85	600	646	0.341	1283.8 ± 15.7	-	0.60
R6	5.23^{t}	5.11^{t}	200 $^{\$}$	1323	65 ± 2 Pt	0.98	900	921	0.742	21.1 ± 2.2	0.64	0.62
R7	5.15^{t}	5.22^{c}	200 $^{\$}$	1323	95 ± 2.5 Pt	0.96	300	321	0.365	31.3 ± 3.7	0.69	0.65
R9	4.83^{t} 4.81^{b}	4.82^{b}	200 $^{\#}$	1323	92.5 ± 2.5 Pt	0.96	420	441	1.0123	14.7 ± 1.6	0.80	0.77
R10	4.84t 4.80^{b}	4.83^{t}	200 $^{\#}$	1323	60 ± 1 Pd	0.98	1200	1221	0.335	26.5 ± 2.7	0.81	0.77

Experiments using same sample are presented in the order in which they were performed. Sphere radii were determined before incorporation in the glass.

C_F refers to the Faxen correction.

Supscripts t, b and c at water contents refer to measurements of slabs from the top, the bottom and the center of the cylinder, respectively. An additional subscript IR is used to distinguish infrared spectroscopy from KFT analyses.

* Experiments performed in piston cylinder apparatus, all others were carried out in IHPVs.

$ Hydrogen fugacity of 6.4 bar during synthesis and in the experiment.

Hydrogen fugacity of 20 bar during synthesis and in the experiment.

Table 3. Results of parallel plate viscometry at 300 MPa

Sample	Temperature (K)	log η exp.(Pa·s)	Fe^{2+}/Fe_{tot}	H_2O (wt%)
MDIB7	747	10.33	0.70	3.3
	757	10.07		
	747	10.36		
	768	9.77		
	747	10.47		

Table 4. Total iron contents in run products using AuPd capsules.

Sample	Temperature (K)	Microprobe FeO_{tot} (wt%)	Colorimetry FeO_{tot} (wt %)
MDIB 25	1523	7.34	7.07
MDIB 30		7.74	7.39
MDIB 31	1473	7.71	7.39
MDIB 32		7.66	7.73

Figure 1

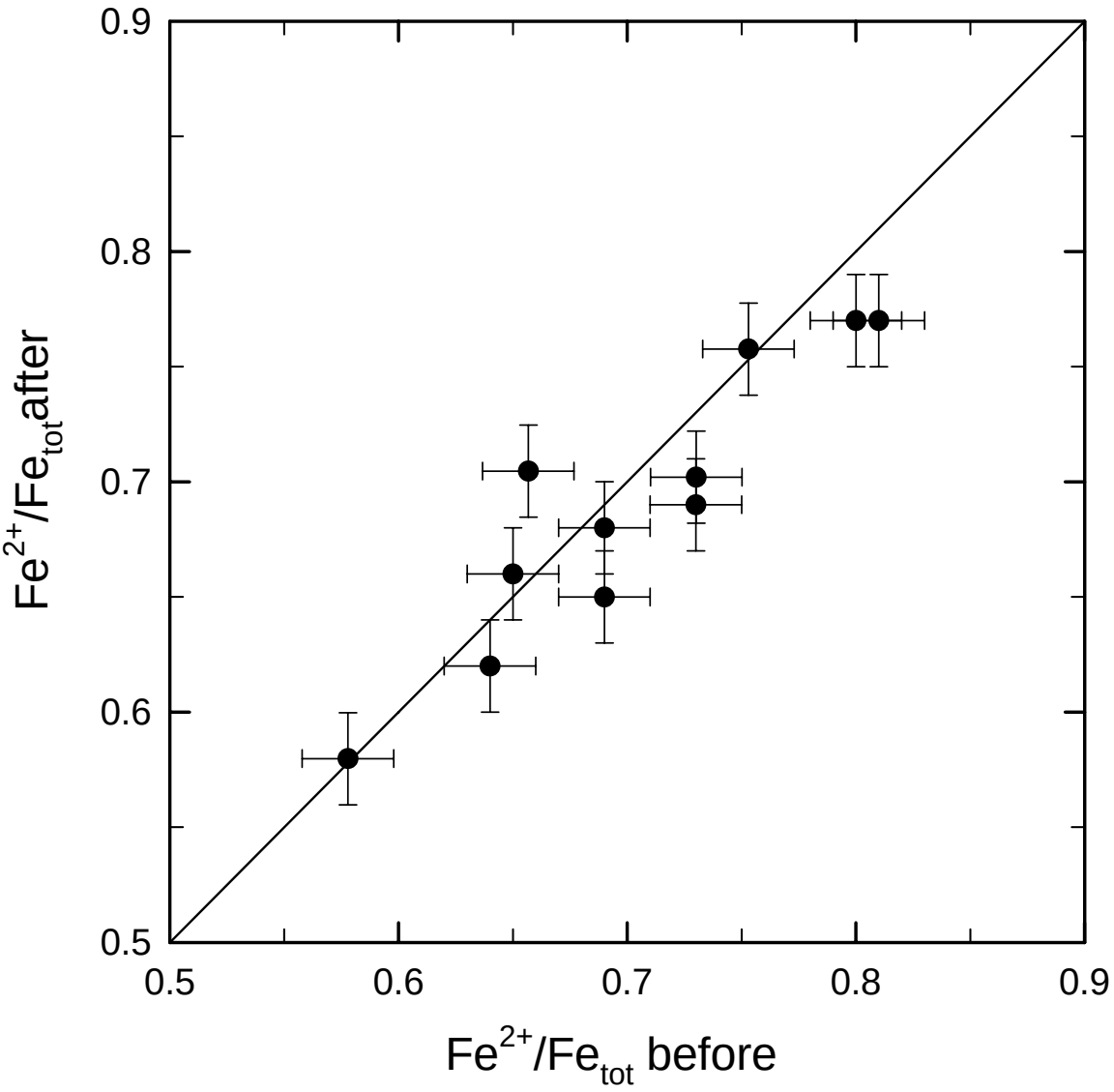

Figure 2

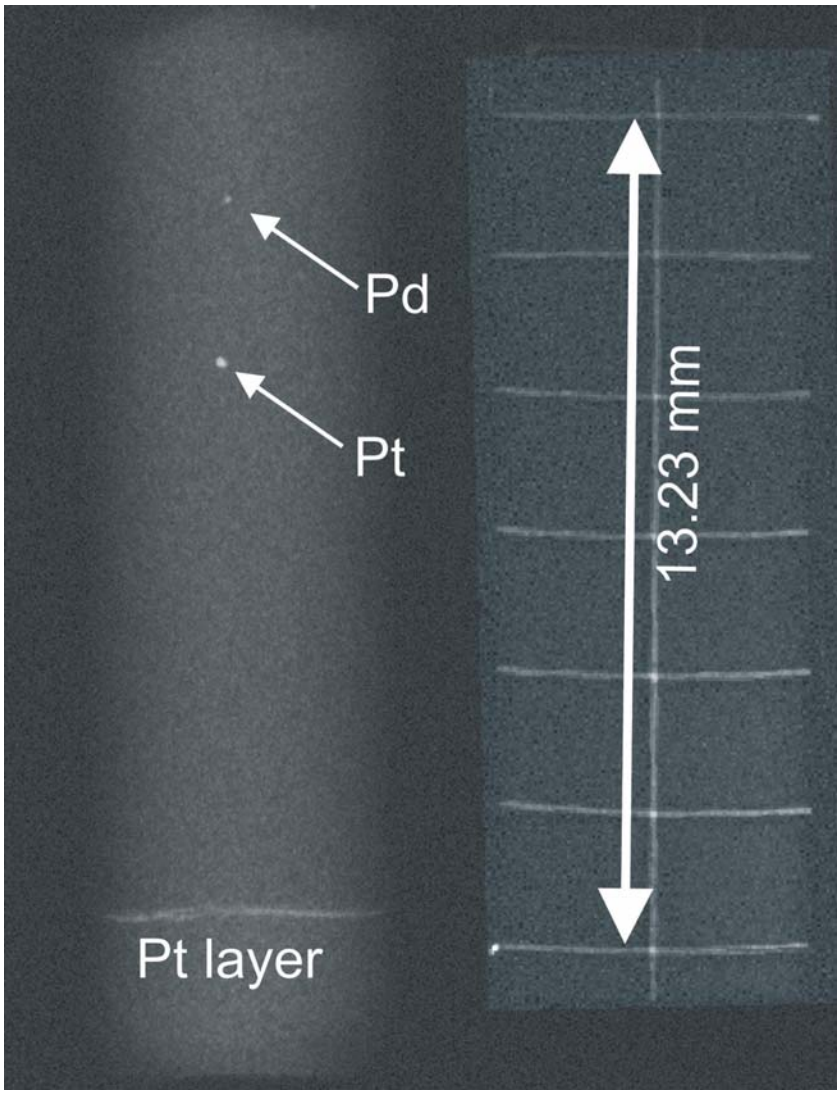

Figure 3

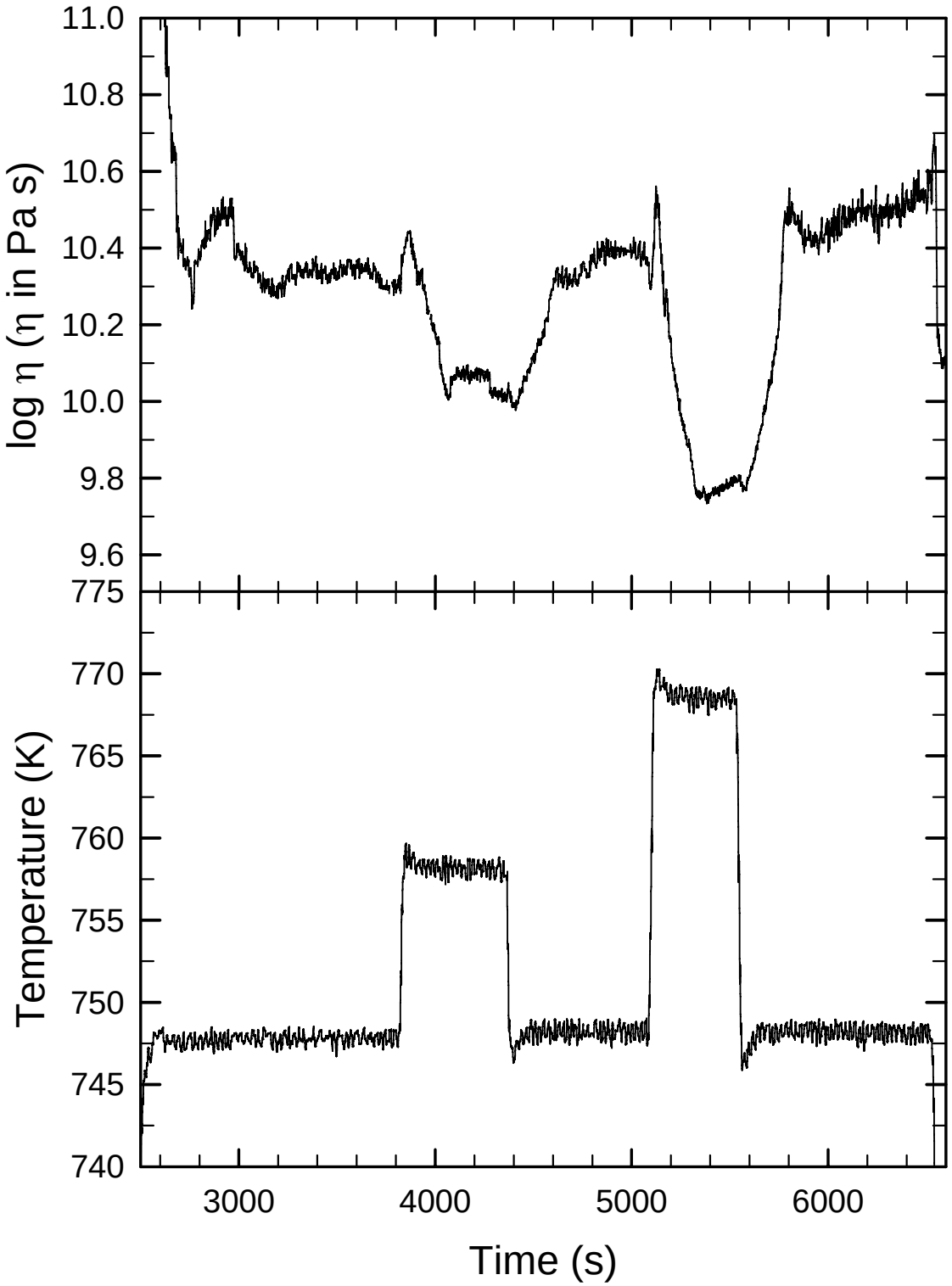

Figure 4

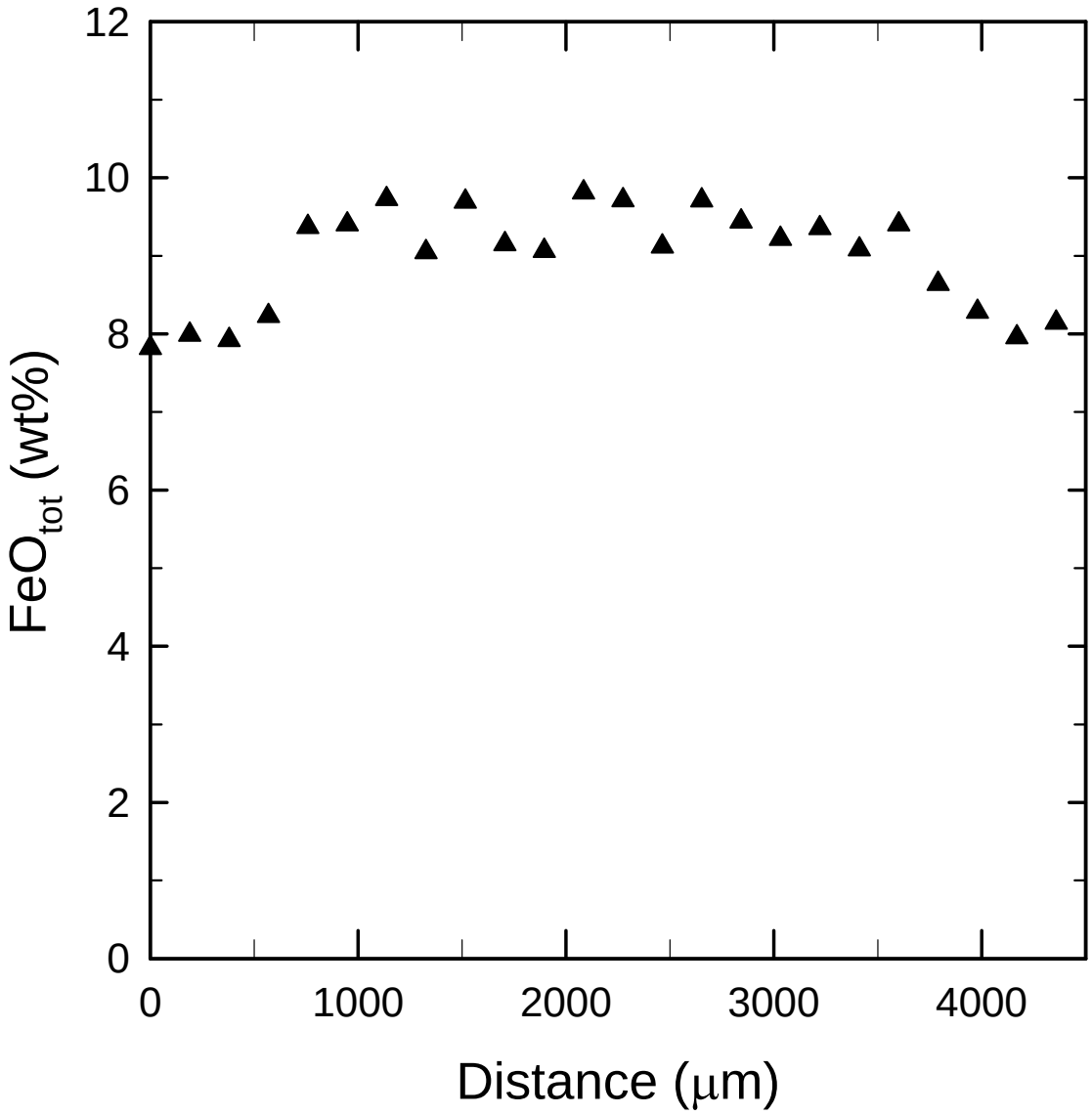

Figure 5

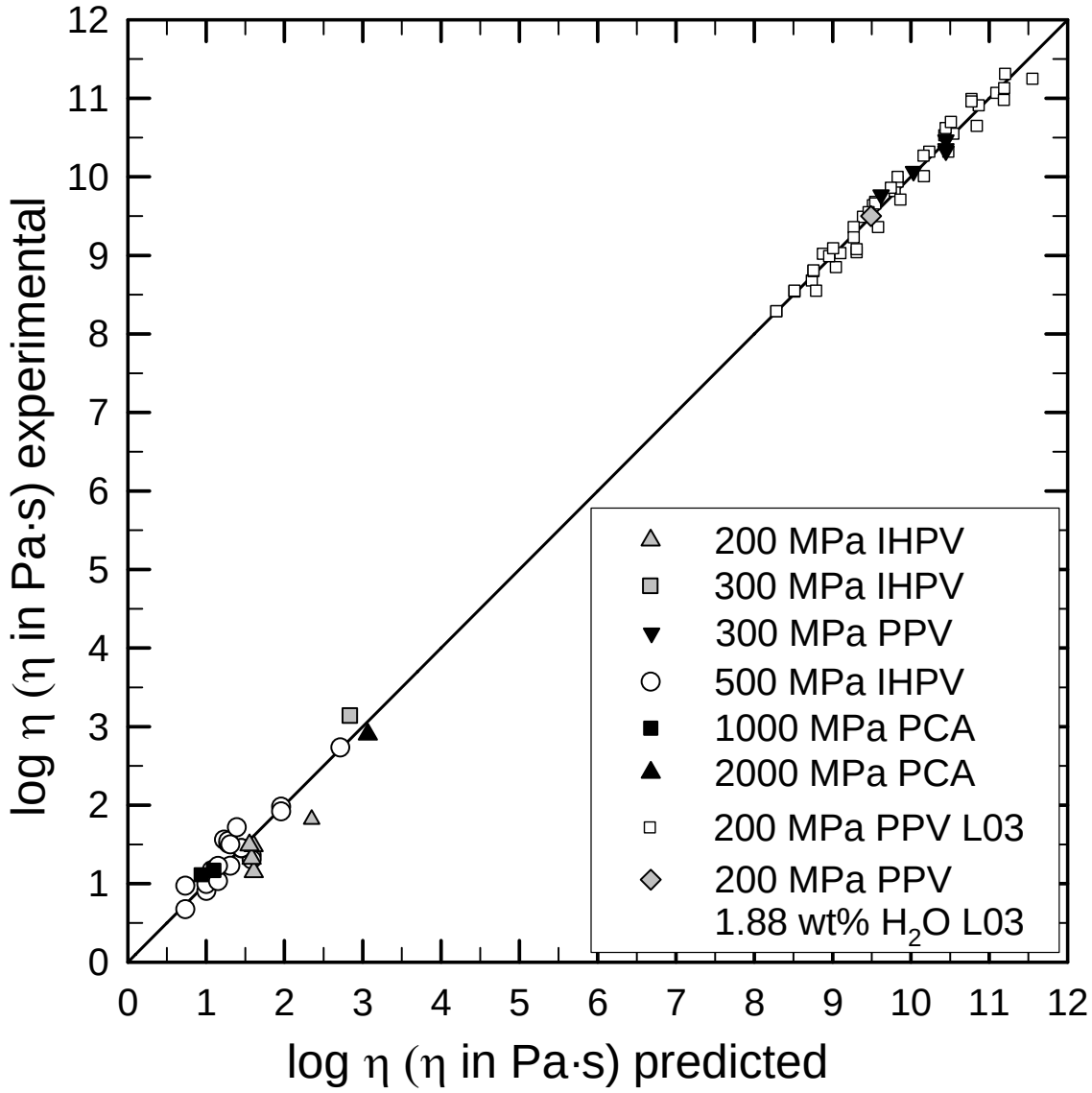

Figure 6

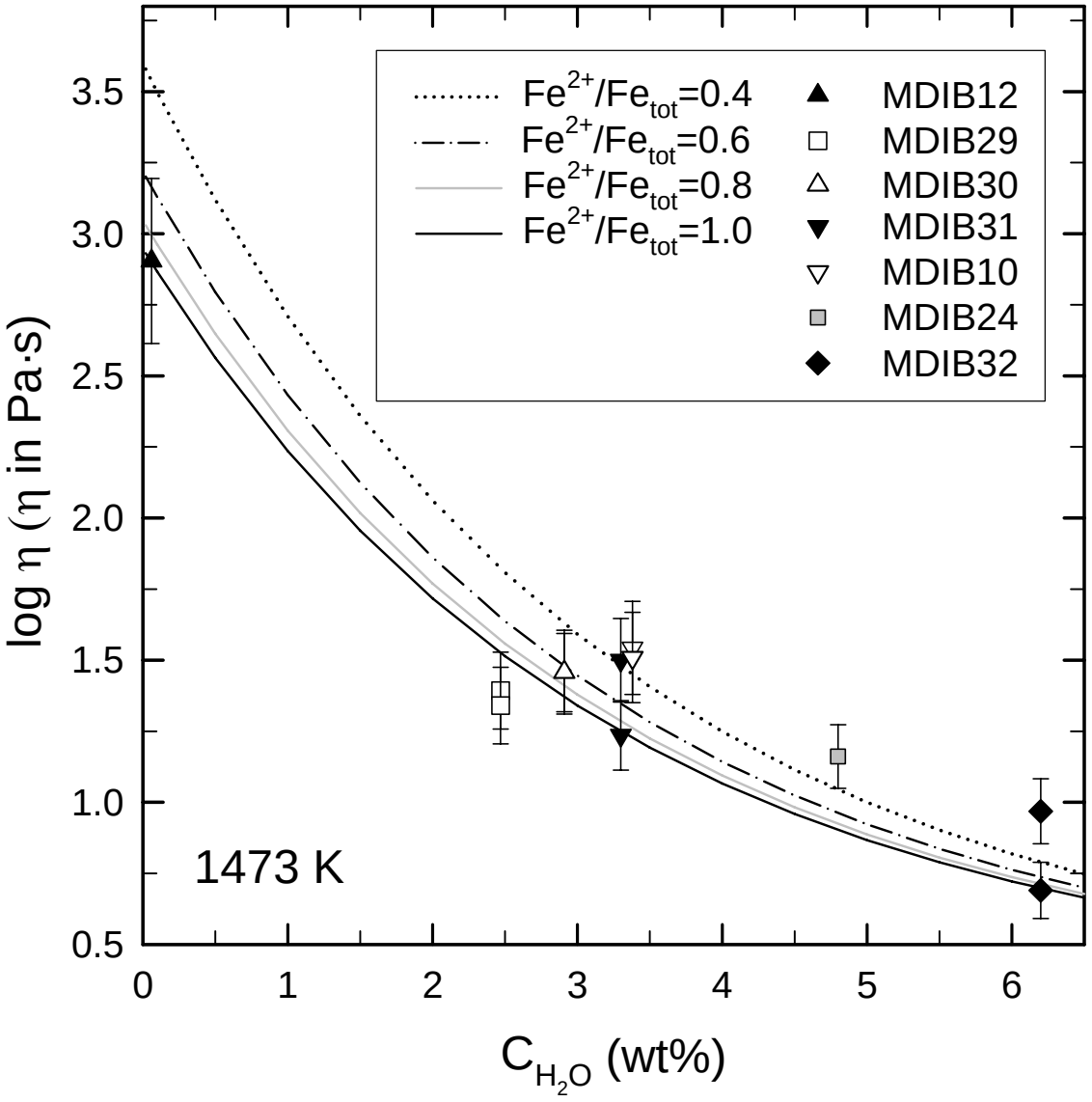

Figure 7

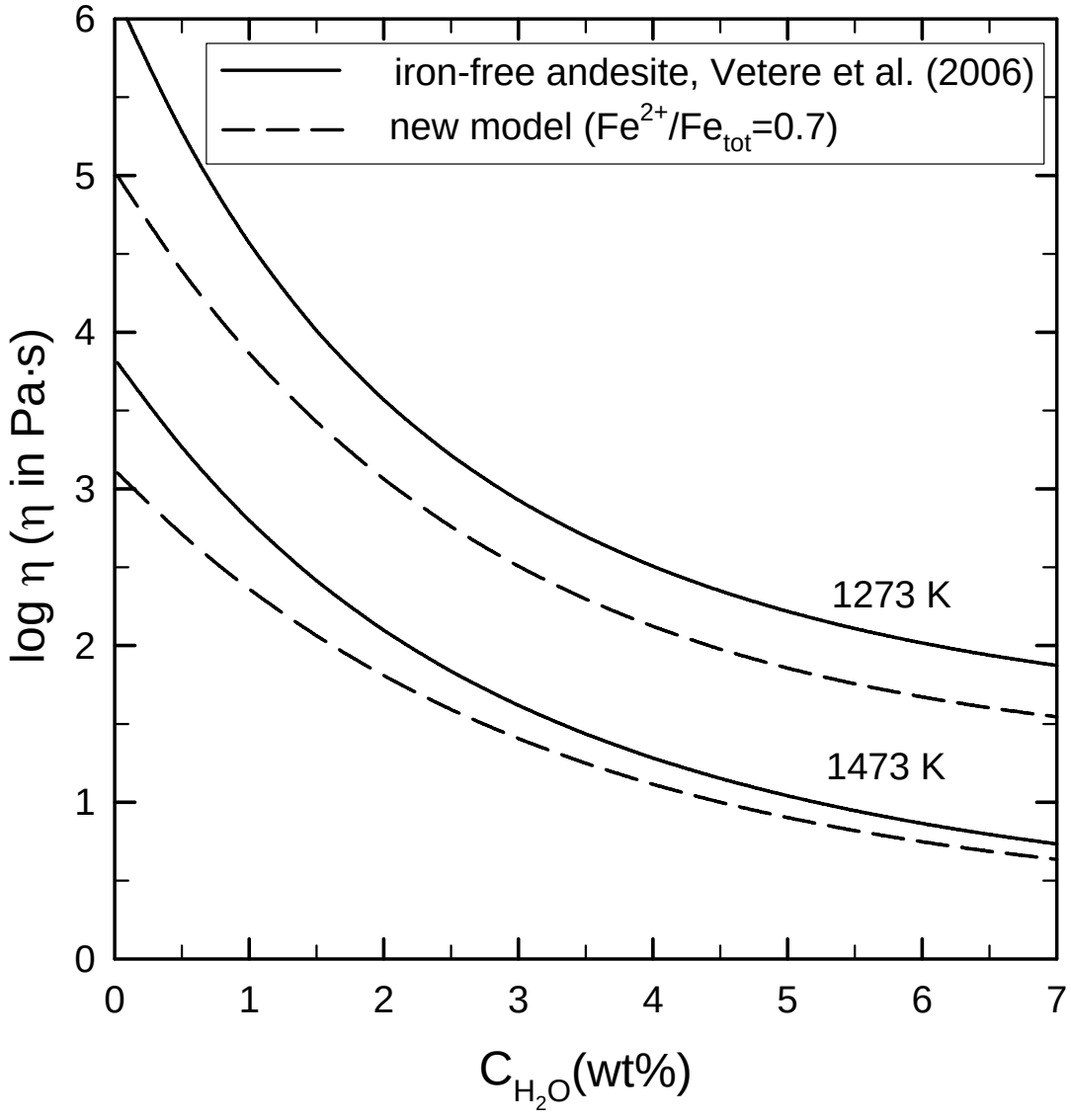

Figure 8a

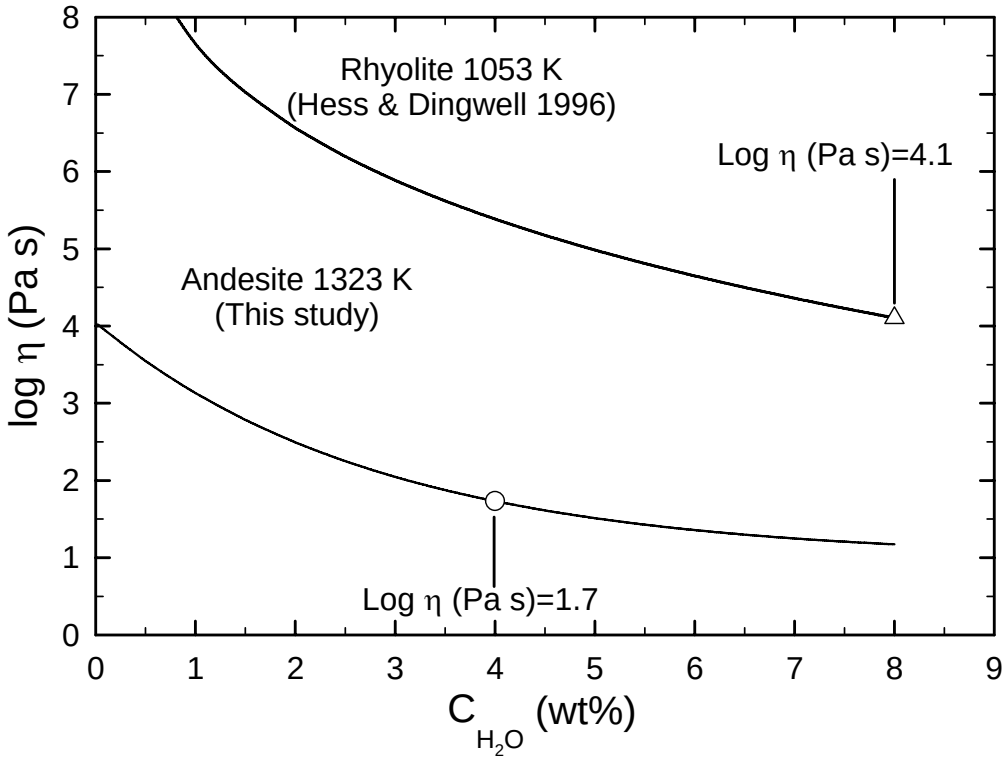

Figure 8b